GEOPHYSICAL RESEARCH LETTERS, VOL. 23, NO. 5, PAGES 455-458, MARCH 1, 1996

Crustal shear-wave splitting from local earthquakes in the Hengill triple junction, southwest Iceland

John R. Evans
U. S. Geological Survey, Menlo Park, California

G. R. Foulger
Department of Geological Sciences, University of Durham, U. K.

Bruce R. Julian
U. S. Geological Survey, Menlo Park, California

Angus D. Miller
Department of Geological Sciences, University of Durham, U. K.

Abstract. The Hengill region in SW Iceland is an unstable ridge-ridge-transform triple junction between an active and a waning segment of the mid-Atlantic spreading center and a transform that is transgressing southward. The triple junction contains active and extinct spreading segments and a widespread geothermal area. We evaluated shear-wave birefringence for locally recorded upper-crustal earthquakes using an array of 30 three-component digital seismographs. Fast-polarization directions, ϕ, are mostly NE to NNE, subparallel to the spreading axis and probably caused by fissures and microcracks related to spreading. However, there is significant variability in ϕ throughout the array. The lag from fast to slow *S* is not proportional to earthquake depth (ray length), being scattered at all depths. The average wave-speed difference between *qS1* and *qS2* in the upper 2-5 km of the crust is 2-5%. Our results suggest considerable heterogeneity or strong *S* scattering.

Introduction

The Hengill ridge-ridge-transform triple junction in SW Iceland links the Western Volcanic Zone (WVZ), a waning NNE-striking segment of the mid-Atlantic ridge, the Reykjanes Peninsula Volcanic Zone (RPVZ), an en-echelon array of short spreading segments, and the South Iceland Seismic Zone (SISZ), a complex transform zone extending east across south Iceland to the Eastern Volcanic Zone (EVZ) (Figure 1, inset). The SISZ consists of rotating blocks bounded by north-striking strike-slip faults producing destructive earthquakes [*Einarsson*, 1991; *Stefánsson et al.*, 1993]. In the triple junction the ridge jumped ~5 km west at ~0.5 Ma [*Foulger*, 1988]. The area now contains the actively spreading Hengill system and extinct Grensdalur system, each comprising a central volcano, fissure/fault system, and geothermal area. A third system (Hrómundartindur) lies between Hengill and Grensdalur. It developed in the ridge-migration period but never into a full spreading segment.

In 1991, 30 portable seismographs were operated at a total of 33 sites (Figure 1) in the 25×25 km Hengill area [*Foulger et al.*, 1995], principally to study non-shear earthquakes that occur there [*Foulger*, 1988]. The network had three-component 2-Hz velocity sensors and 16-bit digital recorders. It recorded several thousand local microearthquakes. We also use data from the nearest station (BJA) of the permanent 1-Hz South Iceland Lowland (SIL) network, which spans the SISZ [*Stefánsson et al.*, 1993]. The data are suited to studying shear-wave birefringence, the splitting of *S* into orthogonally polarized quasi-phases *qS1* and *qS2*. The polarization direction of the faster *qS1*, ϕ, may imply crack or foliation orientation; the time lag $t_{qS2} - t_{qS1}$ may constrain crack densities.

Shear waves from local earthquakes recorded by SIL stations show evidence of crustal anisotropy [*Menke et al.*, 1994]. Most ϕ are NE, except near the Hekla volcano (at the east end of the SISZ) and near some strike-slip faults north of the SISZ. Lags of 100 to 300 ms imply upper crustal shear-wave speed anisotropy of 7-12% and crack densities of up to 21%. Here we use our data to resolve details of shear-wave splitting in a smaller area at the west end of the SISZ, an area of diverse tectonic units and widespread high-temperature geothermal resources.

Data and Method

We measured shear-wave splitting on 237 three-component seismograms from 120 microearthquakes. These were selected from the data set of *Foulger et al.* [1995] solely according to the "shear-wave window" (keeping incidence angles at the surface less than critical to quell particle-motion complications). To determine the window, and incidence angles at the surface, we use their (*L2*) best-fit one-dimensional v_P model and their v_P/v_S ratio, derived from a modified Wadati diagram. The data set of *Foulger et al.* [1995] was selected in turn from the thousands recorded on the basis of record quality, measured by the number and quality of picks from an automatic picker. We further limited our data set to those with good evidence of birefringence, as follows.

The seismograms are sampled at 100 samples per second (sps)—somewhat coarsely. Since the REFTEK recorders used yield rigorously unaliased data, we applied a phase shift to remove the acausal effects of the anti-alias filters (J. Fowler, personal communication, 1993) then interpolated the records from 100 to 800 sps (FFT, pad between Nyquists with zeros, inverse FFT). Both processes proved helpful in identifying and measuring ϕ and the arrival times of *qS1* and *qS2*. This improvement is in the analyst's ability to make visual identification and correlations of waveforms, and in the ability to pick small lags to less than than one sample interval of the original.

We used particle-motion plots to find approximately linear, horizontal *S* motion followed by more complex motion [e.g., *Zhang and Schwartz*, 1994], and visually analyzed these records with the PITSA software system [*Scherbaum and Johnson*, 1993]. First we verified nearly horizontal particle motion at t_{qS1} *via* three-dimensional particle-motion plots, then determined ϕ

Paper number 96GL00261
0094-8534/96/96GL-00261$03.00

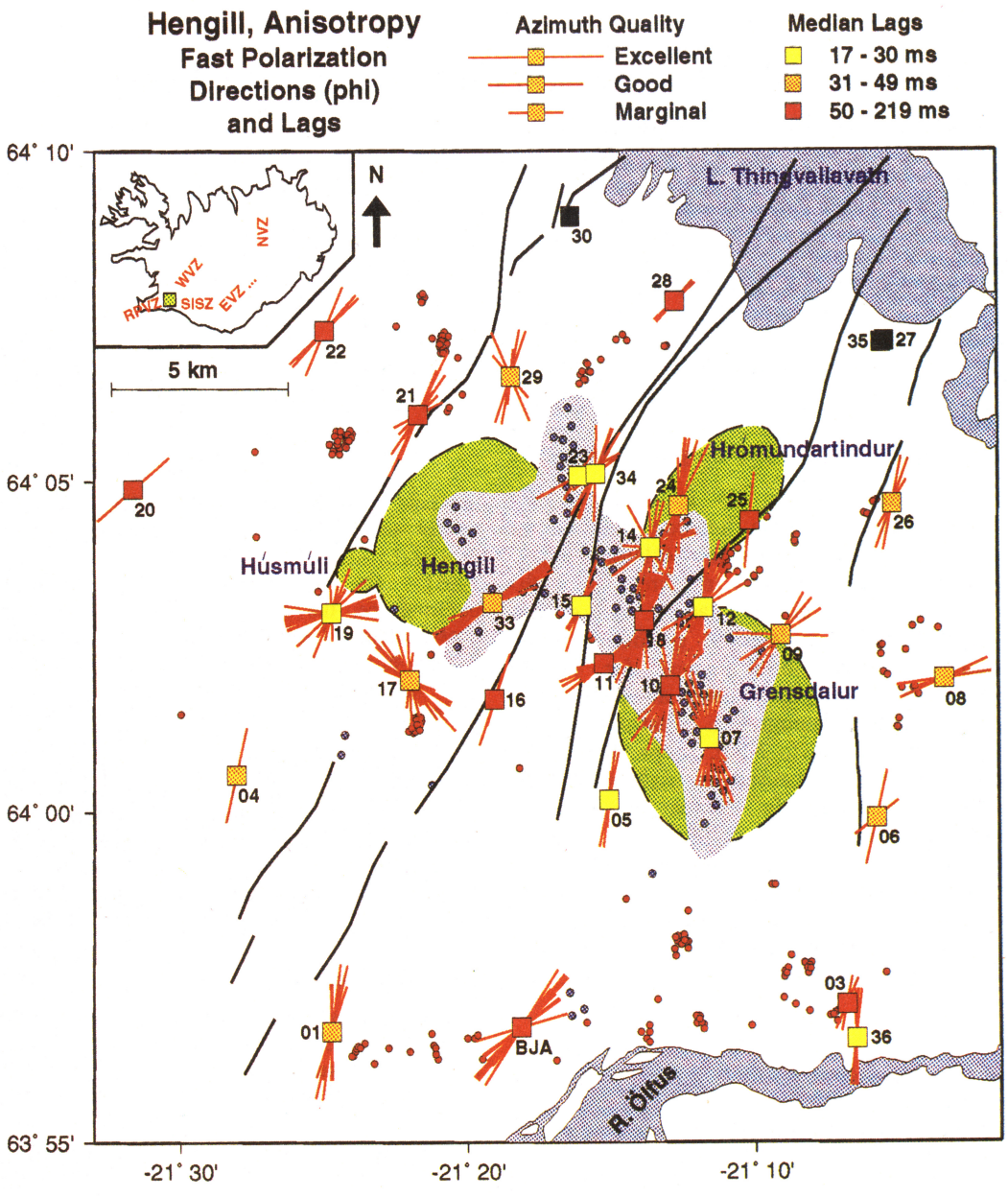

Figure 1. Stations used (squares) and observed ϕ, red lines. Line length: ϕ quality; colors of squares: median lags, $t_{qS2} - t_{qS1}$; light blue: geothermal field; blue dots: thermal springs; red dots: earthquakes used; green shading: volcanoes; black lines: fissure swarm boundaries. Inset: area of map and regional tectonic zones. RPVZ. WVZ, EVZ, NVZ: Reykjanes Peninsula, Western, Eastern, and Northern volcanic zones; SISZ: South Iceland Seismic Zone.

in plots of the horizontal-plane, rotated in-plane to this direction, and finally measured t_{qS1} and t_{qS2}. Each of these three measurements, ϕ, t_{qS1}, t_{qS2}, was classed subjectively as "Excellent", "Good", or "Marginal". Examples of each grade of record are shown in Figure 2. About 63% of the records examined yielded viable pick triples, with 43% of these having ϕ, t_{qS1}, and t_{qS2} all rated "Good" or better. The vertical components of "Good" and "Excellent" records offer little evidence of *S*-to-*P* converted precursor phases. In contrast, many "Marginal" records are contaminated by clear precursor phases or, for unknown reasons, have nonhorizontal *qS1* motion.

Results

Most ϕ measurements at a given station are narrowly clustered, and most lie in the NE to NNE direction (Figures 1 and 3; Table 1), subparallel to the trend of the spreading plate boundary and of most surface faults and fissures. However, ϕ varies throughout the network, often by large amounts over short distances (e.g., station 17 *vs* 33, BJA *vs* its neighbors, 11 *vs* 18). A few stations have widely scattered ϕ (e.g., 14 and 19). This complexity is reflected in Figure 3, which has at least two prominent peaks. The complexity does not seem to decrease with distance from the central volcanoes. Lastly, there may be correlations between ϕ at some stations and linear groups of nearby thermal features, notably at station 07.

Our one SIL station, BJA, deserves comment. We observe strongly peaked ϕ with a median value of N42°E (we use medians throughout the paper to obviate outliers). *Menke et al.* [1994] report ϕ "strongly peaked at N30°E" at BJA, though their Figure 6*a* shows a range from about N20°E to N60°E. In either case, BJA contrasts with neighboring stations.

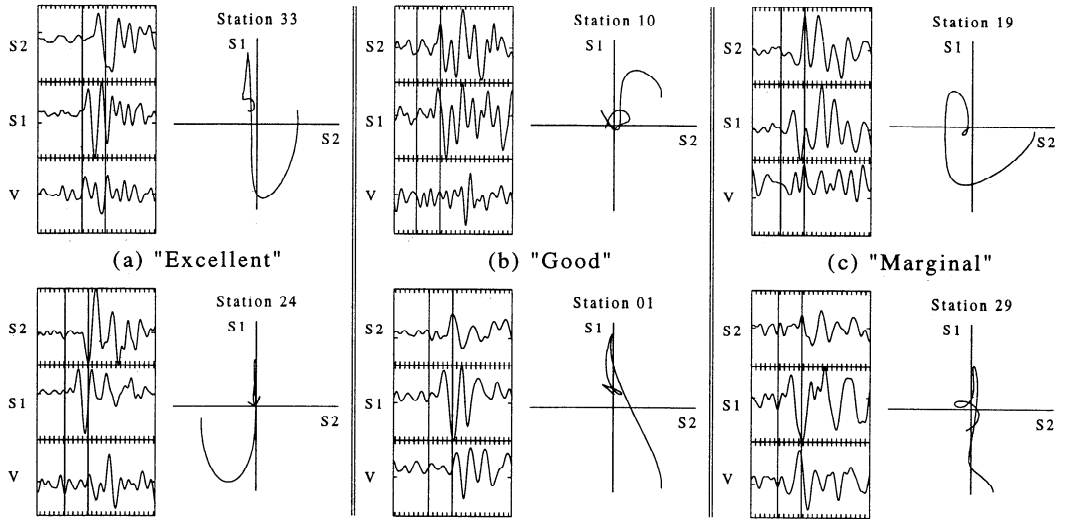

Figure 2. Data examples, with horizontals rotated to ϕ. A 0.5-s window centered near *qS1* is shown, with relative amplitudes preserved. Horizontal particle-motion plots are of the 0.1-s subwindows shown by vertical lines. Examples of (*a*) the best records (ϕ, t_{qS1}, t_{qS2} all "Excellent"), (*b*) "Good" records, (*c*) "Marginal" records.

The $t_{qS2} - t_{qS1}$ lags have a median of 40 ms for the whole data set, *vs* 100 to 300 ms reported by *Menke et al.* [1994] for the SIL network. They report lags of ~50-150 ms for BJA (their Figure 6*a*); our median is 53 ms. This discrepancy may be due to (1) longer path lengths used by *Menke et al.* [1994], (2) their use of cross-correlation, which might find *qS2* better in the presence of scattered *S*, (3) our stations being near active volcanoes, or (4) 10-ms granularity in the values of *Menke et al.* [1994] (they evidently worked at 100 sps). The dominant sources are likely to be the reading method and siting near volcanoes. Indeed, nearly all of our smallest lags (yellow squares, Figure 1) are near the central volcanoes.

Figure 4 shows lags *vs* focal depth (roughly proportional to ray length since incidence angles are limited). Few values are as large as those of *Menke et al.* [1994], and those over 150 ms are questionable. There is no clear variation of lag with depth, though the scatter appears largest near the median focal depth (4.7 km) and smaller at both depth extremes. We did not explore correlations with other variables, such as backazimuth.

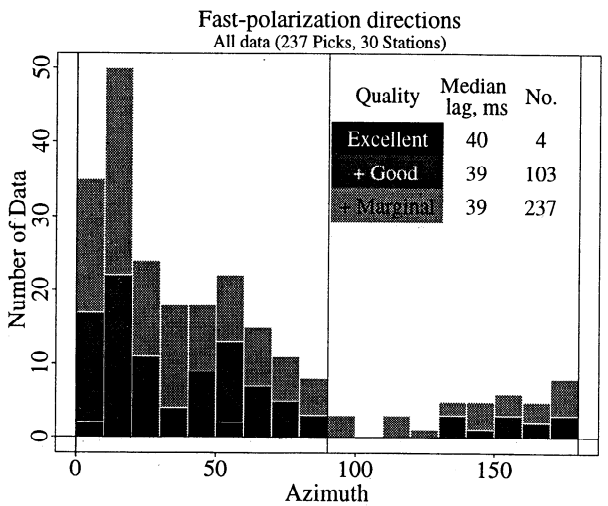

Figure 3. Histogram of ϕ for the full data set. Median $t_{qS2} - t_{qS1}$ lags are given with the number of data contributing.

Assigning the median lag to a vertical ray from 4.7 km deep gives an "average" shear-wave speed anisotropy of 2.4%; attributing it to only the upper 2 km gives 4.6%. However, the large scatter of lags suggests that anisotropy is spatially heterogeneous or that scattered *S* obscures *qS2* [*Aster et al.*, 1990].

Table 1: ϕ and $t_{qS2} - t_{qS1}$ lag by station

Station	Number of data	median ϕ (°)	σ_ϕ* (°)	median lag (ms)	σ_{lag}* (ms)
01	7	11	7	35	10
03	2	18	9	50	21
04	1	13	–	44	–
05	3	7	4	26	13
06	2	32	28	41	38
07	12	178	16	17	16
08	4	72	7	46	3
09	4	50	27	36	23
10	17	19	16	54	28
11	8	65	12	82	49
12	24	16	13	24	27
14	11	17	39	19	12
15	3	28	8	18	73
16	2	18	1	72	46
17	17	144	21	44	27
18	18	18	9	66	28
19	20	76	28	19	7
20	1	49	–	108	–
21	6	34	15	78	39
22	4	44	11	219	104
23	2	47	21	25	23
24	12	8	7	40	17
25	2	6	1	51	30
26	3	20	10	47	5
28	2	44	5	70	2
29	5	6	25	41	10
33	19	58	5	40	19
34	8	26	17	18	15
36	4	2	3	26	13
BJA	14	42	10	53	24

*σ means the (*L2*) standard error.

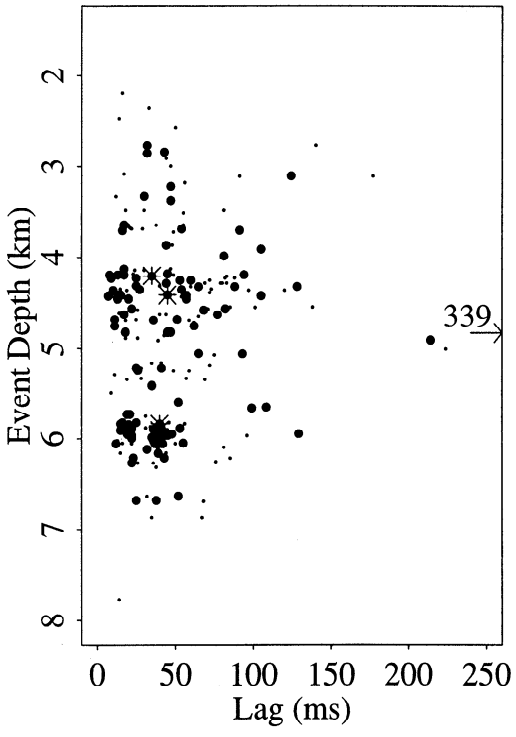

Figure 4. Focal depth (from sea level) *vs* lags, $t_{qS2} - t_{qS1}$. Larger dots all "Good" or better; stars: all "Excellent"; arrow: only datum outside plot. Mean station elevation 339 m.

Discussion

The EDA (extensive dilatancy anisotropy) hypothesis [*Crampin*, 1978], attributing anisotropy to stress-induced subvertical fractures and microcracks, provides the most likely explanation of our results. For *S* propagating in the plane of the cracks, wave speed is faster for particle motions polarized parallel to the fractures. Surface fissure and dike alignments, tectonic grain, and microearthquake focal mechanisms [e.g., *Klein et al.*, 1977; *Foulger*, 1988] suggest ridge-perpendicular extension. The direction of maximum horizontal compression may rotate with depth, but T-axes of focal mechanisms remain horizontal and ridge perpendicular [*Klein et al.*, 1977]. EDA cracks would strike about N25°E, consistent with Figure 3 (median ϕ of N21°E). Other foliations, like dike orientations and flow alignment of crystals within dikes, also may contribute to the observed anisotropy.

There is some suggestion in Figure 1 of a systematic variation in ϕ across the array, from NE in the NW part to NNE in the east and south parts of the array. It would be no surprise if the direction of σ_3 varied around this evolving triple junction. However, variability of ϕ on shorter length scales precludes demonstrating, let alone interpreting, subtle regional trends.

Menke et al. [1994] report significant deviations from NE ϕ near the Hekla volcano. It is to be expected that the stress field, and thus crack directions, are inhomogeneous near volcanoes [e.g., *Nakamura*, 1977]. For the Hengill-Grensdalur complex, surface fissures, dikes, topographical features, and lines of hot springs have strikes ranging from NW to NE. *Foulger* [1988] cited these variations as evidence that radial stress fields locally modify the regional stress field. Add to this that the triple junction is unstable, with variations in ridge azimuth and rotating blocks in the SISZ, and one anticipates complexity.

The lag scatter suggests spatial heterogeneity, but complex structure also scatters *S*, which *Aster et al.* [1990] show can obscure *qS2*. Small lags near the volcanoes suggest lower porosity or increased scattering. Low porosity can be caused by hydrothermal fracture cementation, a thinner brittle (EDA) zone, or fracture annealing. Low lags, the generally NE to NNE ϕ, and complexity in ϕ and lag are the main patterns we find.

Conclusions

Strikes of EDA cracks in the Hengill triple junction, inferred from *S* birefringence, are mostly sub-parallel to the strike of the spreading plate boundary (N25°E). Large station-to-station ϕ contrasts imply a heterogeneous stress field overprinting regional spreading-ridge stress. The ϕ reported by *Menke et al.* [1994] are consistent with our findings, including at the one station in common, BJA. However, we find smaller lags, implying lower porosity or greater scattered-*S* effects in our study. Lag scatter implies either spatially heterogeneous fracture porosity or errors in identifying *qS2*, perhaps due to scattered *S*. Regional spreading-ridge stress is clear, but with major local complexity.

Acknowledgements. This research was supported by the USGS Geothermal Program (JRE and BRJ) and a USGS G.K. Gilbert Fellowship (BRJ). ADM is supported by a Ph.D. studentship from the UK National Environmental Research Council. We thank John Vidale and Mary Lou Zoback (for USGS) and two anonymous GRL reviewers for their helpful reviews of this manuscript. We also thank David Booth, Russ Evans, Xiangyang Li, Colin MacBeth, Aaron Martin, Bob Nadeau, John Orcutt, Wolfgang Rabbel, and Martha Savage for valuable input. Figure 1 was made with the "GMT System" [*Wessel and Smith*, 1991].

References

Aster, R.C., P.M. Shearer, and J. Berger, Quantitative measurements of shear wave polarizations at the Anza seismic network, southern California: implications for shear wave splitting and earthquake prediction, *J. Geophys. Res.*, *95*, 12,449–12,473, 1990.

Crampin, S., Seismic wave propagation through a cracked solid: polarization as a possible dilatancy diagnostic, *Geophys. J.R. Astron. Soc.*, *53*, 467–496, 1978.

Einarsson, P., Earthquakes and present-day tectonism in Iceland, *Tectonophysics*, *189*, 261–279, 1991.

Foulger, G.R., Hengill triple junction, SW Iceland: 2. Anomalous earthquake focal mechanisms and implications for processes within the geothermal reservoir and at accretionary plate boundaries, *J. Geophys. Res.*, *93*, 13,507–13,523, 1988.

Foulger, G.R., A.D. Miller, B.R. Julian, and J.R. Evans, Three-dimensional v_P and v_P/v_S structure of the Hengill triple junction and geothermal area, Iceland, and the repeatability of tomographic inversion, *Geophys. Res. Letters*, *22*, 1309–1312, 1995.

Klein, F.W, P. Einarsson, and M. Wyss, The Reykjanes Peninsula, Iceland, earthquake swarm of September 1972 and its tectonic significance, *J. Geophys. Res.*, *82*, 865–888, 1977.

Menke, W., B. Brandsdóttir, S. Jokobsdóttir, and R. Stefánsson, Seismic anisotropy in the crust at the mid-Atlantic plate boundary in southwest Iceland, *Geophys. J. Int.*, *119*, 783–790, 1994.

Nakamura, K., Volcanoes as possible indicators of tectonic stress orientation—principle and proposal, *J. Volcanol. Geotherm. Res.*, 2, 1–16, 1977.

Scherbaum, F., and J. Johnson, *Programmable Interactive Toolbox for Seismological Analysis, PITSA, Version 4.0, 11-20-93*, Incorporated Research Institutions for Seismology, Data Management Center, Seattle, 1993.

Stefánsson, R., R. Böðvarsson, R. Slunga, P. Einarsson, S. Jokobsdóttir, J. Bungum, S. Gregersen, J. Havskov, J. Hjelme, H. Korhonen, Earthquake prediction research in the South Iceland Seismic Zone and the SIL Project, *Bull. Seismol. Soc. Am.*, *83*, 696–716, 1993.

Wessel, P., and W.H.F. Smith, Free software helps map and display data, *Eos, Trans. AGU*, *72*, 441, 445–446, 1991.

Zhang, Z., and S.Y. Schwartz, Seismic anisotropy in the shallow crust of the Loma Prieta segment of the San Andreas fault system, *J. Geophys. Res.*, *99*, 9651–9661, 1994.

J.R. Evans and B.R. Julian, U.S. Geological Survey, 345 Middlefield Rd, MS-977, Menlo Park, CA 94025.

G.R. Foulger and A.D. Miller, Department of Geological Sciences, University of Durham, DH1 3LE, U.K.

Received: October 2, 1995 Revised: January 16, 1996
Accepted: January 16, 1996